https://doi.org/10.2352/ISSN.2470-1173.2017.6.MOBMU-295

Liquid Crystal lens characterization for integrated depth sensing and all in focus imaging application

Simon Emberger, Laurent Alacoque, Antoine Dupret, Capucine Lecat--Mathieu de Boissac ; CEA Leti ; Grenoble ; France
Jean Louis de Bougrenet de la Tocnaye ; Optics department ; Telecom Bretagne ; Brest ; France
Nicolas Fraval ; Evosens ; Plouzané ; France

Abstract

Depth from focus (DfF) algorithms rely on a scene-invariant series of images captured at different focuses to evaluate the distance between objects of the scene and the camera. One limitation of this technique is the slight "focus zoom" caused by standard lenses where focus is achieved with lens translation. Focus zoom impacts the performance and complexity of DfF estimation algorithms because it requires a costly spatial transform for images registration. Liquid Crystal (LC) lenses and liquid lenses do not rely on lens translation for focus which makes them good candidates for processing-inexpensive DfF techniques. On the other hand, DfF distance resolution depends on the number of acquired images under the constraint of scene-invariance which, in turn, calls for fast framerates and hence fast focusing. LC lenses are not the fastest lenses technology available and a careful characterization of both control vs. focus and focus speed is therefore required in order to define the acquisition system specifications. This paper presents both a system and a method to control and characterize a focus tunable lens. We developed a dedicated methodology, driver and algorithms to control experimental LC lenses in order to evaluate their compliance with the application and compare them with commercial-off-the-shelf (COTS) liquid lenses. Our experimental system controls, captures and processes images to measure the speed limitation of these lenses. We discuss the LC lenses performances, compare them with liquid lenses and show an example of depth map extraction with both of these lens technologies.

Introduction

2D imaging constitutes a lossy projection of an actual scene. In embedded computer vision, the trend is to get ever richer information from the scene. The depth of the scene is a direct extension of visual information and many works provide solutions for this application. In order to provide an estimation of the depth, efficient 'active' solutions exist. For instance time of flight measurement [1] is already widely used but, as most of solutions, is not adapted to low-power applications. Stereoscopy is a well-known 'passive' solution but calibration issues make it of impractical use in a processing-limited embedded environment. Alternatively, depth maps can also be computed by analyzing the level of blur of a single image of the scene using depth from defocus (DfD) methods. It is achieved at the expense of an important post-processing [2-4]. Other techniques deduce depth maps from the sharpness variations of images captured during a focus sweep (depth from focus: DfF) [5-7]. This technique has the advantage of being 'passive' and to require limited computation power and a standard focus lens. This approach is hence suitable for embedded processing. Two challenging optical devices families exhibit promising performances for this application: Liquid Lenses [8, 9] which are already commercially-available and experimental Liquid Crystal Lenses [10]. The latter exhibits desirable form factors (thinness and size) and a large focal power dynamic without any mechanical translation. The purpose of this paper is to propose a simple methodology for in-system characterization of tunable lenses and to conclude on their performances for DfF applications. Key parameters for DfF applications are evaluated and a simple example of depth maps extraction is presented.

Following sections present the hardware and test environment, algorithms designed for parameters characterization and the analysis of focal zoom.

Characterization system

Figure 1 shows the architecture used for lens characterization. It is composed of a tunable lens and its driver, a camera module with an image sensor and a fixed focal lens, a GPU & CPU platform or a computer and a display.

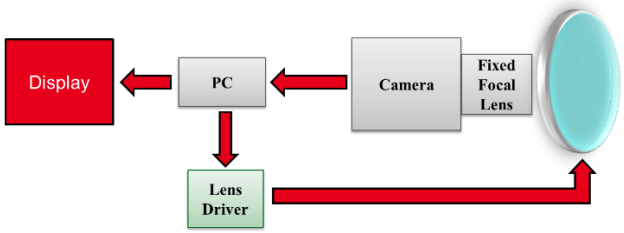

Figure 1. Characterization system architecture

Tunable lenses

Tunable lenses are lenses which have the ability to change their focus distance without any mechanical translation. In fact, for many image processing this translation movement impacts acquired images because it induces a zoom effect which has to be compensated by computing-expensive image registration. In this paper, this phenomenon is referred to as "focal zoom". Since tunable lenses do not have to move to change its focus, this effect should be much reduced. Furthermore, we might expect that this kind of lenses show faster focus variations than mechanical ones. The aim of this paper, is to provide a first validation of these assumptions. The rest of this section presents two families of tunable lenses that we are comparing in this paper and the way to control them.

Liquid Crystal lens

A LC lens is made of a thin layer of Liquid Crystal surrounded by two electrodes. By applying an electric field in the LC layer, the crystal molecules spin round and the optical index is locally changed which affects the wave front and hence the optical properties of the device [10-12].

More recently, some low-aberration, homogenous LC lenses were developed [10]. These experimental lenses are presented on Figure 2 and characterized below.

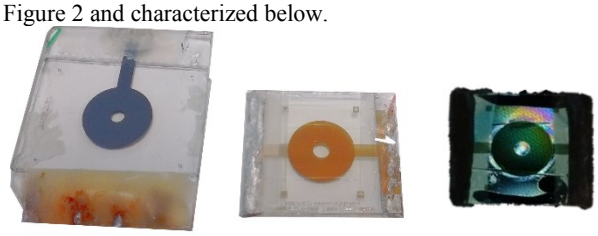

Figure 2. Experimental LC lenses from [10]: 2 mm aperture, clear and polarized 2.5 mm aperture

LC lenses are made of two glass substrates coated with a resistive solution and circular metallic electrodes. The substrates are aligned and spaced at a calibrated distance using micro balls, thus determining the thickness of the inner nematic LC layer.

The focal power exhibit a large evolution scale which is advantageous for DfF applications.

LC lenses are birefringent devices. By applying an electrical field to the nematic layer, only one of its two optical indexes evolves. For this reason, LC lenses exhibit focus power along the extraordinary direction only. Since our purpose is to use it with common light and image sensor, two choices come out:

- use a system made out of two lenses and oriented with two orthogonal axes
- use one lens and a polarizer

The first solution is better according to the photon ratio collected on the sensor. On the other hand, the limited precision of lenses alignment and the slight distance that exists between the two aligned lenses reduces the lens aperture and requires slightly different commands. This causes calibration and focus-tuning issues. For these reasons, a one-lens with polarizer was characterized in this paper.

LC lens driver

The lens is controlled using a symmetric AC signal. Focus sweep is obtained by varying the AC frequency and/or the polarization voltage. To keep the lens driver simple, a frequency-only controller was preferred. The easiest way to generate variable frequency signal is using pulse width modulation (PWM). A driver is needed to adapt required amplitude to 5-15V and keep lens DC polarization level to 0. In fact, higher voltage are suitable for this kind of lenses but since we aim at an embedded solution, we chose to limit it to achievable voltages.

Several solutions can be adapted for the command: H-bridges, comparators or amplifier based designs. H-bridge is probably the most elegant solution because it allows an output swing twice the voltage of the power supply and H-bridges relies on passive elements. One drawback of this solution is that switches phases need non-overlapping control which are not easily generated from a single ended clock. Indeed, ill-synchronized phases can produce short-circuits and damage the system. To simplify prototyping, we choose a comparator-based driver as a level shifter. The LM239 is well adapted for two main reasons. Thanks to its open drain output, which only needs a pull up resistor to bring Vcc_h, it limits the power of Vcc_h source. It also support frequency higher than 200 kHz which should not be a limit for LC lens polarization. To get a symmetric signal we chose to create a fictive reference centered at $Vcc_h/2$. The lens is connected between this reference and the comparator output. Figure 3 shows a schematic of the LC lens driver.

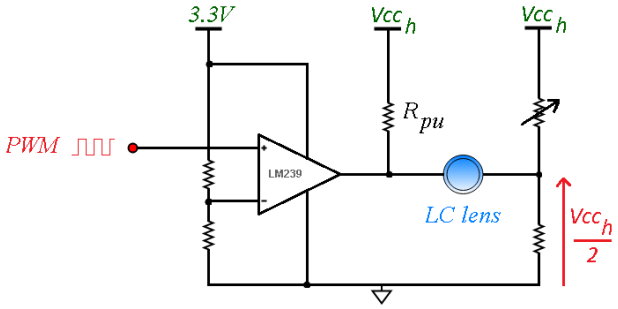

Figure 3. LC Driver level-shifter electrical schematic

The PWM signal is generated by a STM32 microcontroller operated using and USB UART link. This was chosen because of its programmability, and real-time features and it can be used to issue a pair of control signals for orthogonal-lenses solutions in future experiments.

Optotune's Liquid lenses

To validate our algorithms, we chose to use two commercially available Optotune lenses. They are made of two immiscible transparent liquids with different refractive indexes. Applying an electric field allows to bend the membrane between the two phases which allows to tune their focal power. Due to their commercial availability, theses lenses are well calibrated and easily controllable using dedicated serial protocol configurable lens driver. This makes it a very practical solution for comparison because it is close to our experimental setup and easy to implement.

Camera modules

To characterize the lens without the requirement of a dedicated optical bench, one can rely on an image sensor and a lens for direct image acquisition. Due to the technology-limited pupil diameter of LC lenses, an aperture-adapted micro-camera should be chosen. Moreover, as stated before, both the application and the lens speed characterization require a high frame-rate camera. These criterions lead us to choose the Leopard Imaging MT021C module which is a 60fps camera with raw output. In order to avoid the aperture reduction, lenses must be placed as close as possible from the camera fixed-focal lens. For this reason, a dedicated 3D stand was designed. It is presented on Figure 4.

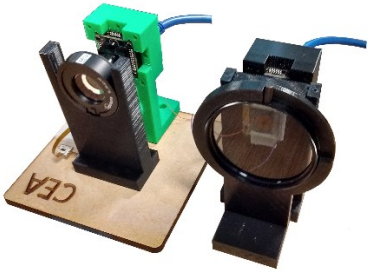

Figure 4. Two complete optical system, with the both kinds of lenses. 16 mm Optotune Liquid lens (left) 2.5 mm experimental LC lens behind a polarizer (right)

For LC lenses characterization, a polarizer is added in front of the camera in order to align the light beam polarization along the privileged axis of the lenses. The camera built-in lens is manually tuned to focus to infinity when the tunable lenses are turned off.

Experimentation

We compare two experimental LC lenses with two liquid lenses from Optotune. Their main characteristics are presented in Table 1.

Table 1: Lenses parameters

Lens	LC 2	LC 2.5	EL-10-30-C	EL-16-40-TC
Pupil (mm)	2	2.5	10	16
Thickness (mm) Active layer (µm)	3 18	1 125	24.6 4400	11.9 N/A
F min (cm)	20	20	20	33
F max	∞	∞	∞	∞
Δn	0.26	0.26	N/A	N/A
Δε	12	12	N/A	N/A
Viscosity (m.Pa. s)	203	203	N/A	N/A

Both liquid lenses show bigger 10 mm and 16 mm pupils than LC lenses but are also much more voluminous.

Calibration algorithms and results

The purpose of the algorithms presented in this section is quadruple: finding the speed limit of LC lenses, calibrating them, evaluate the focal zoom amplitude and comparing these characteristics with liquid lenses. Characterization algorithms were written in C and OpenCV 3 in order to maintain portability among hardware version of the central computing platform. Executable are run under the Linux operating system (OS).

LC lenses require an initialization sequence in order to obtain optimal working conditions. For this, a 250 Hz ± 10V voltage is applied to the lens during a short 2 s delay. This allows to activate the LC molecules and avoid nonlinear effect such as disclination lines as explained in [10].

Focused Distance vs. command

DfF relies on a series of images acquired for various distances of focus. For each pixel of the output image, DfF algorithm select the most focused image for this pixel; the estimated distance is deduced from the distance of focus of the selected image. For this, the relation that links command and distance of focus must be carefully characterized. Moreover, a criterion for image selection must be chosen. One prominent criterion family for focused image selection is the sharpness. Sharpness is an image-local criterion that heavily depends on the image content and shows an extremum when the lens is focused. In the literature, several contrast-based analysis methods were presented [13, 14]. A low-complexity, easy to implement sharpness criterion is required in order to implement it efficiently. We so chose to use the difference between the maximum and minimum of the cropped image Laplacian.

Figure 5 presents a flowchart of our calibration algorithm. For each point of the characterization, a high-contrast target is placed at a known distance of the camera. Then, contrast evaluation is performed on a preselected evaluation area for different commands and the command that provides the sharpest image is deduced for the current target distance. Additionally, acquisition noise is reduced by averaging N consecutive images for each characterized distance. To evaluate the efficiency of this algorithm, we first tested it with the liquid lenses. Both of them are controlled by Optotune integrated USB driver using focal power control parameter.

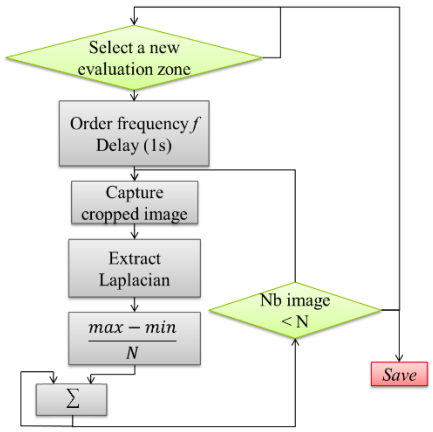

Figure 5. Distance- focus characterization algorithm for LC lenses

We expect to find experiment points distance d_o which fit with the equation (1)

$$d_o = \frac{d_i \cdot f_{fixed}}{d_i + d_i \cdot f_{fixed} \cdot f_p (1 - e) - f_{fixed}} \quad (1)$$

with d_i, the distance between the lens and the sensor, f_{fixed} the fixed focal of the camera lens, e the space between the two lenses and f_p the focal power of liquid lenses.

In theory, with a camera fixed-lens focused at infinity and the two lenses really close to one another, $f_{fixed} = d_i$ and $e = 0$. So the black curve should represent multiplicative inverse. Since Optotune lenses are not extremely thin and the camera is not focused exactly at infinity, we had to fit f_{fixed} and e to obtain the theoretical (black) curve. Figure 6 shows the theory curve and the two experimental ones corresponding to the two Optotune lenses.

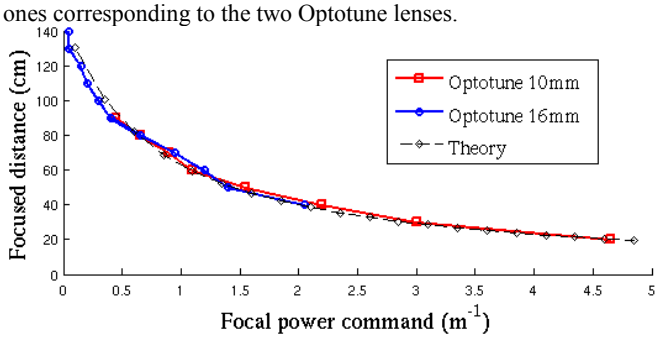

Figure 6. Focused distance computed with the algorithm vs. command focal power for the two Optotune lenses

The measured points fit with the theory when $e = 0.7\ mm$ and $f_{fixed} = 7.957$ mm which correspond to a focus point of $1.45\ mm$ instead of the infinity. This difference can be explained by the small aperture of the camera lens which reduces the hyperfocal distance and the unprecise manual setup of the fixed lens. This proves the ability of our method to correctly evaluate the focus point.

Identical measurements were conducted for the LC lenses. They are presented on Figure 7. The best focus-speed vs. system embeddability tradeoff for the Vcc_h polarization voltage was found to be 20V. This can be improved by tuning the Δε.

As it can be seen, although much more compact, LC lenses exhibit focal powers range close to those of liquid lenses.

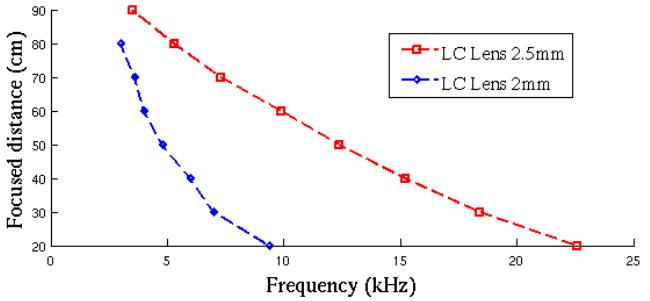

Figure 7. Focused distance versus LC lens polarization frequency with Vcc_h=20V

Focus speed characterization

As stated above, real time DfF applications require fast tunable focus. Characterizing the focus speed is therefore mandatory for system performances evaluation. To evaluate focus speed, a focus-stabilization criterion must be found. We based our criterion on frame to frame difference. When the focus is stable in a controlled environment, image difference is only caused by scene changes and pixel noise. On the other hand, during a focus change, the focus blur constantly evolves and impacts the frame to frame difference. Figure 8 shows the algorithm used to determine the LC lens stabilization speed.

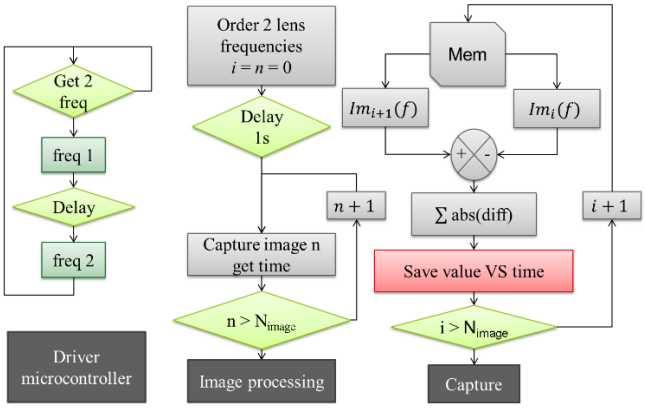

Figure 8. Lens stabilization speed measurement algorithm: capture phase (left) and criterion calculation phase (right)

Because of the non-real time nature of the PC operating system, we found it more robust to acquire N_{image} images as a whole raw video of the focus change and use post-processing to analyze the focus change. Additionally to frequency synthesis, frequency jump timings were implemented in the driver microcontroller to ensure reproducible real-time operation.

The acquisition phase controls the acquisition of the images and the focus change between two focus points. In this phase, a first frequency is applied to LC lens and the video acquisition starts when the first focus point is stabilized. During video acquisition a second frequency is applied to the LC lens which allows to measure focus variations. After video acquisition, the focus analysis phase begins. In this phase (Figure 8, right) the absolute sum of frame to frame differences of a high contrast region of interest is performed to determine focus-variation amplitude.

We found out that the focus variation criterion is very sensitive to illumination variations and therefore requires a light-controlled environment.

Figure 9 shows the evolution of our focus variation criterion versus time for 2.5 mm LC lens for two opposite focus changes.

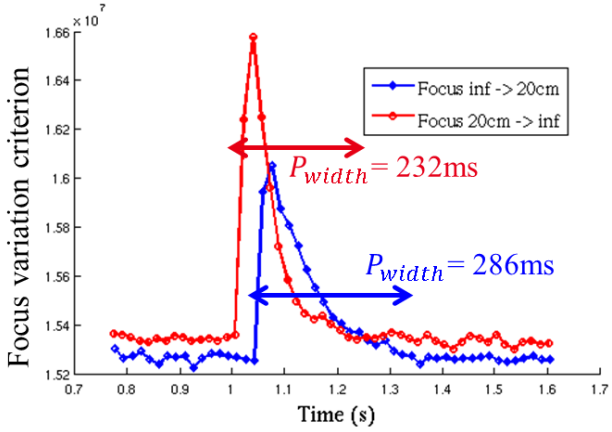

Figure 9. Focus speed measurements for 2.5 mm LC lens.

As it can be seen, the focus change clearly appears after the STM32 wait time delay (1s approx. depending on the video start time). Stabilization time is measured by computing the peaks width P_{width}.

This method is sufficient for high-speed cameras or slow lenses but problems can arise for faster lenses or slower cameras. Figure 10 illustrates the case where focus variation is of the same order of magnitude than image integration time.

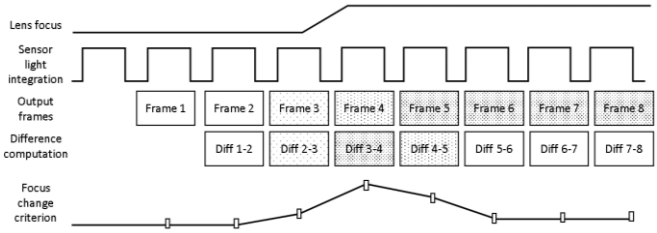

Figure 10. Detail of speed measurement when the focus variation time is closed to the integration times

Intuitively, when the focus changes during a time frame of one image period, one could expect a single point peak for the criterion, but as it can be seen on Figure 10, the fact that the focus variation can't be synchronized with image integration time impacts the measurement. On Figure 10, a short focus change overlaps two frame integrations, resulting in a three different frames sequence. Focus change criterion being based on frame difference, this results in a four frame-differences sequence and thus impacts the computed peak width to 2 to 3 consecutive non-null points. Finally, the focus variation time T_{focus} can be approximated by equation (2) with P_{width} the measured width of the peak, I_{time} the image integration time on the sensor (16ms at 60 fps).

$$P_{width} - 4 \cdot I_{time} < T_{focus} < P_{width} - 2 \cdot I_{time} \quad (2)$$

The focus speed measurements for the four lenses are summed up in Table 2. The first number is the focus delay for a nearer focus and the second number is the focus delay for a farer focus. Optotune lenses data marked with an asterisk were extracted from the lenses

datasheet. LC lenses data marked with a dash were not measurable due to the limited focus range of the 2 mm pupil LC lens.

Table 2: Summary of the speed measurements

Focus step (cm)	40↔70	40↔90	70↔90	Max
LC 2mm (ms)	52 68	- -	- -	110 76
LC 2.5mm (ms)	98 117	108 133	52 77	254 200
Opto 10mm (ms)	10* 6*	10* 6*	10* 6*	10* 6*
Opto 16mm (ms)	15* 15*	15* 15*	15* 15*	15* 15*

As it can be seen, Optotune lenses show faster focus speed than LC ones. This is somewhat compensated by the (not represented) configuration delay of the lens USB driver which makes it insufficiently reactive for real-time DfF applications with fast cameras.

In this experiment, focus speed of the LC lenses was impacted by the nematic layer large thickness. The large thickness was needed to allow for large aperture and hence depth resolution, but it has a direct negative impact on the lens speed. In future lens design, we will tune the LC solution towards higher Δn and lower viscosity to allow for thinner faster lenses with the same aperture.

On the driver point of view, the speed of the LC lenses could also be augmented with a higher Vcc_h, but in this paper, we are limited by the LC driver components maximum voltage, this can also be improved by raising the Δε parameter of the nematic layer.

Focal zoom characterization

Focal zoom represents the amount of zoom effect observed when the focus changes. For focal zoom measurement, a scene presented on Figure 11 was set up.

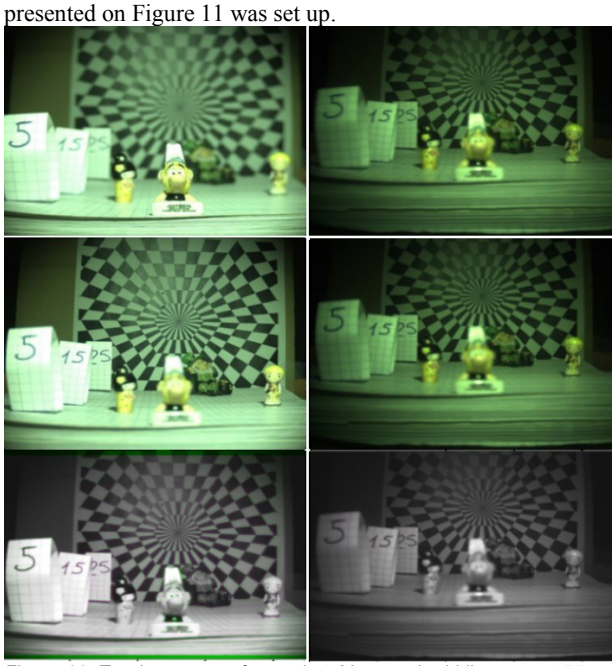

Figure 11. Top images are focused at 20cm and middle ones at 55cm. The bottoms ones show the scale difference by superposition. The left side pictures were acquired with 10 mm Optotune lens and the right pictures were acquired with 2.5 mm LC lens.

A polarizer was used even with liquid lenses but the LC lenses smaller pupils is responsible for the observed luminance difference. At first sight, the focal zoom is difficult to see, except with the slight crop of picture on the image boundaries. Optotune lens (left) focal zoom is more noticeable than LC lenses (right). To quantitatively measure the focal zoom, we used Matlab imregister tool using a 'similarity' transform type. Scale factors were extracted from the resulting tForm structures. Translation, rotation and shear factors were consistently measured to be close to zero. To avoid uncertainty caused by very different images, we chose to capture 8 to 10 images with slight focus changes instead of a min-max focus image pair only. For each consecutive image pair, the focal zoom was extracted using imregister function and accumulated to calculate the total focal zoom of the lens. Figure 12 represents the cumulative zoom factor of each of the four lenses.

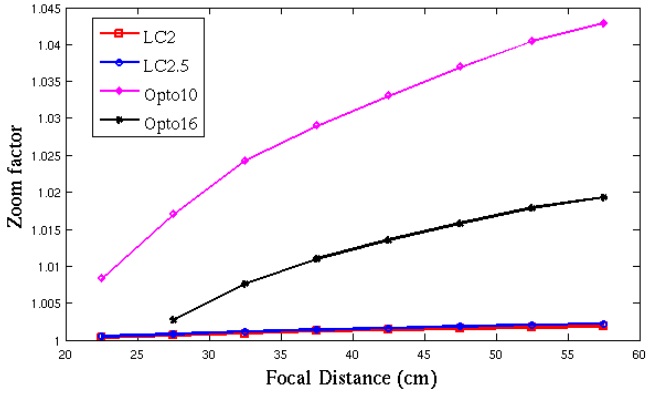

Figure 12. Cumulated Zoom factor versus Focused distance.

As it can be seen, the focal zoom of the LC lenses is less than 0.25% for the whole focus range. On the other hand, Optotune lenses exhibit larger focal zooms of 1.15% and 4%. Smaller zoom factors greatly facilitates image registration step needed by DfF by reducing the lookup neighborhood. With a very limited scale factor, LC lenses offer the advantage to completely avoid the requirement of this registration step.

Depth Map and All in Focus image extraction

To evaluate the potential of these lenses for DfF application, an algorithm of depth map extraction based on Laplacian was designed. This algorithm was preferred to more recent methods because of its low-complexity for embeddability reasons. The Laplacian dynamic in a scare 16x16 area is used as a contrast criterion like the previous calibration algorithm. Depth extraction is computed by selecting the focus image with highest contrast criterion. Raw extraction results are shown on Figure 13.

Optotune lenses produce better depth images in this specific case. This is due to the fact that the small-aperture LC lenses don't provide short-enough depth of fields for focus selection. In addition to smaller apertures, diffusion of light due to the LC layer overlarge thickness has a negative impact on local contrasts and hence depth-sensitivity. The thicker the LC layer, the more diffuse the light: this accounts for an additional source of blur that impacts sharpness criterion and hence the DfF sensitivity. Again, this will hopefully be improved by tuning Δn and Δε parameters to allow for thinner LC lenses. Finally, for greater fairness, contrast criterions less sensitive to LC light diffusion should be evaluated.

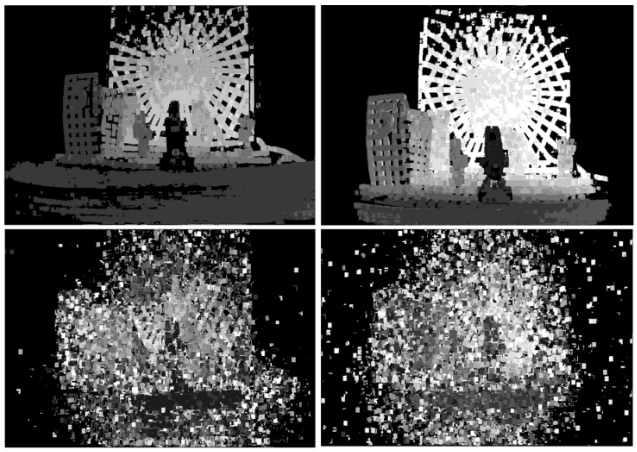

Figure 13. Depth map extracted with the four lenses, Optotune 16 mm and 10 mm (top) and LC 2.5 and 2 (bottom). The darker, the nearer.

All-in-focus images are reconstructed from the image cube and depth map. Figure 14 presents the corresponding all in focus images.

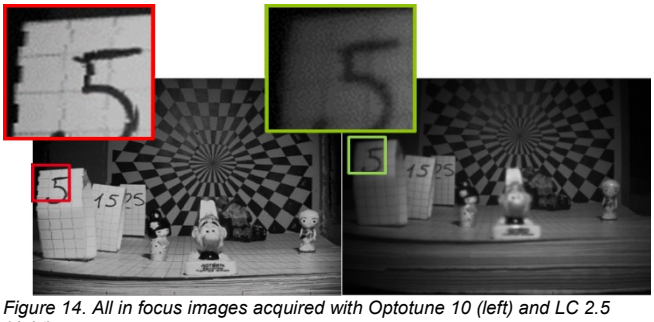

Figure 14. All in focus images acquired with Optotune 10 (left) and LC 2.5 (right)

Each pixel of the image is replaced by pixels coming from the best image according to the depth map. Some artifacts show up for Optotune's lens (see cropped image). These artifacts are due to the focal zoom, they appear on the Optotune all in focus images but the quality remains good. LC lenses are not impacted with this issue but lack some contrast, once again because of light diffusion.

Conclusion and perspective

In this paper, we proposed a method to characterize the distance of focus vs. control frequency, the focus speed and the focal zoom of liquid and liquid crystal lenses without the need of state of the art optical testbench. Four lenses of Liquid Crystal and Liquid technologies were tested. LC lenses are more compact than Liquid ones for comparable focus range. Regarding focus speed, LC lenses are 10 to 50 times slower than liquid lenses which could be a problem for high speed DfF applications. Focus zoom was characterized. As expected, both liquid and liquid crystal lenses offer a very limited zoom over the full focus range. In this regard, LC lenses perform 4 to 15 times better than liquid ones. Depth map extraction shows that the LC diffusion is an issue for embedded DfF application because it limits the LC lenses contrast. Meanwhile it was discussed that nematic viscosity and optical anisotropy might be tuned to improve contrast and speed performances of LC lenses.

References

[1] Hach, Thomas; Steurer, Johannes; Knob, Sascha, Electronic Imaging, 3D Image Processing, Measurement (3DIPM), and Applications 2016, pp. 1-9(9), High-Fidelity Time-of-Flight Edge Sampling Using Superpixels

[2] Chunping Hou Chang Tang and Zhanjie Song. Journal of Modern Optics, 2014. Depth recovery and refinement from a single image using defocus cues

[3] Chang Tang, Chunping Hou, and Zhanjie Song, "Defocus map estimation from a single image via spectrum contrast," Opt. Lett. 38, 1706-1708 (2013)

[4] Anat Levin, Dani Lischinski, Yair Weiss. A closed-form solution to natural image matting. EEE Trans Pattern Anal Mach Intell. 2008 Feb; 30(2): 228–242. doi: 10.1109/TPAMI.2007.1177

[5] Integrated three-dimensional vision sensor. CEA Patent.

[6] C. Liu and L. A. Christopher, "Three dimensional moving pictures with a single imager and microfluidic lens," in *IEEE Transactions on Consumer Electronics*, vol. 60, no. 2, pp. 258-266, May 2014. doi: 10.1109/TCE.2014.6852002

[7] Suwajanakorn, Supasorn and Hernandez, Carlos and Seitz, Steven M., Depth From Focus With Your Mobile Phone The IEEE Conference on Computer Vision and Pattern Recognition (CVPR), 2015, pp. 3497-3506

[8] Franck Fillit Hilario Gaton Martin Guillet Olivier Jacques-Sermet Frédéric Laune Julien Legrand Mathieu Maillard Nicolas Tallaron Eric Simon, Bruno Berge. Optical design rules of a camera module with a liquid lens and principle of command for AF and OIS functions. Proceedings of the SPIE, Volume 7849, id. 784903 (2010)

[9] M. Blum, M. Büeler, C. Grätzel, M. Aschwanden. Compact optical design solutions using focus tunable lenses , SPIE Optical Design and Engineering IV, Proceedings Vol. 8167 (2012)

[10] Nicolas Fraval and Jean Louis de Bougrenet de la Tocnaye, "Low aberrations symmetrical adaptive modal liquid crystal lens with short focal lengths," Appl. Opt. 49, 2778-2783 (2010)

[11] Susumu Sato. Liquid-Cristal Lens-Cells with Variable Focal Length. 1979 The Japan Society of Applied Physics Japanese Journal of Applied Physics, Volume 18, Number 9

[12] Hung-Chun Lin, Ming-Syuan Chen, and Yi-Hsin Lin. A review of electrically tunable focusing Liquid Crystal lenses. TEEM, vol. 12, no. 6, pp.234-240, December, 2011.

[13] S.K. Nayyar and Y. Nakagawa. Shape from Focus: an effective approach for rough surfaces. International Conference on Robotics and Automation, 2:218{225, 1990

[14] E. Krotkov, Focusing, International Journal of Computer Vision, Vol. 1, pp. 223-237. 1987.

Author Biography

Simon Emberger received the Dipl.-Ing (M.Sc.) degree in electrical engineering from ENSEA School, Cergy, France in 2014 and the M.Sc. in autonomous electrical systems engineering (ISIM-ESA) from Université de Cergy Pontoise, Cergy, France, in 2014. He is currently a PhD student in microelectronic and nanotechnology at CEA-LETI. His current research interest includes embedded processing in CMOS smart sensors for depth map extraction.